The Effect of Curing Conditions and Fiber End Shapes on the Mechanical Properties of Composites

AKIN ATAŞ* AND NURETTIN ARSLAN
Balikesir University, Department of Mechanical Engineering, Balikesir, Turkey

SELIM TÜRKBAŞ
Gazi University, Department of Mechanical Engineering, Ankara, Turkey

ZAFER ÖZDEMIR
Maintenance School and Training Center, Balikesir, Turkey

ABSTRACT: The study consists of two main experimental parts. The aim of the first part of the study is to investigate the effects of the straight-short steel fibers and different curing conditions on the mechanical properties of the selected composite specimens. For this purpose, unreinforced (no fiber) specimens cured at room temperature (~20°C) and the straight-short steel fiber reinforced polyester–calcite composite specimens cured at room temperature and at different curing conditions of 40, 80, and 120°C for 4, 8, and 12 h, have been subjected to tensile tests. In the second part of the study, unreinforced specimens and polyester–calcite composite specimens with straight-short, woven, and three different end shaped fibers cured at room temperature have been tested according to the four-point bending test procedure so as to obtain the effects of the end shapes on the mechanical properties of the composite specimens.

KEY WORDS: straight-short fiber, various end shaped fibers, cure conditions.

INTRODUCTION

THE APPLICATIONS OF fiber reinforced composites have grown rapidly and are now widely used in industry. Due to the fact that the fabrication cost of a short fiber composite is considerably lower compared to that for a continuous fiber composite and that the short fiber composite is more feasible from a mass production point of view than is the continuous fiber composite, short fiber composites are finding increased use in commercial applications where weight savings are highly desired. Elementary methods of mechanics are easily applied to continuous fiber systems to predict the strength and structural behaviors. In short fiber composites, the analysis is complicated due to the discontinuities at the fiber

*Author to whom correspondence should be addressed. E-mail: akin@balikesir.edu.tr
Figure 5 appears in color online: http://jrp.sagepub.com

0731-6844/09/21 2665–10 $10.00/0 DOI: 10.1177/0731684408093452

ends and it has been found that high stress concentration occurred at the fiber end [1]. Reinforcing fibers may be long (even continuous) and carefully aligned, or short with only a limited degree of alignment that is produced by flow during fabrication [2].

Short-fiber reinforced composites have many advantages compared to continuous-fiber composites. Recently, there has been considerable interest in the effect of the various end shaped fibers on the mechanical behavior of composite materials. Liou conducted a study about the effects of different geometrical shapes of fiber end, the ratio of fiber length to diameter, the fiber volume fraction and the elastic modulus ratio to the normal, and the interfacial shear stress distributions of short fiber composites [1]. Unusual fiber morphology has recently been proposed in the literature by Zhu et al. [3–8] Bone-shaped short (BSS) fibers and their mechanical properties have been investigated in many articles [3–8]. From these investigations, it is clear that the BSS fibers have better mechanical properties than conventional-straight-short (CSS) fibers. Bagwell and Wetherhold [9] determined the fracture toughness of the end-shaped (straight, flat end-impacted, and rippled) copper reinforced epoxy matrix composites by using a four-point bending test and showed that the flat end-impacted fibers increase the composite's fracture toughness by exactly 46%. Between the reinforcement fibers and matrix materials, weak interfacial properties cause the separation. Optimization of the shape of the fibers can improve load transfer capacity between the fibers and the matrix materials. Zhou et al. [10] improved a procedure for structural shape optimization of short reinforcement fibers using finite-element analyses and demonstrated that a threaded end short (TES) fiber can considerable improve the bonding ability between the fibers and the matrix materials. On the other hand, Zhou et al. [11] have developed an optimization procedure and find that the optimal fiber geometry looks like a dumbell shape when the fiber is perfectly aligned to the loading direction. Jiang et al. [12] experimentally evaluated the effectiveness of bone-shaped short (BSS) steel wire reinforcement in improving the mechanical properties of cement and revealed that BSS steel-wire-reinforced cement is stronger, tougher, and more crack resistant than conventional-straight short (CSS) steel-wire-reinforced cement and unreinforced cement.

In the present study, to obtain the curing condition effects, unreinforced (no fiber) specimens which are cured at room temperature and the straight-short steel fiber reinforced polyester–calcite composite specimens that are cured at room temperature and at different curing conditions of 40, 80, and 120°C for 4, 8, and 12 h, have been subjected to tensile tests. At the same time, unreinforced, straight-short fibers, woven and three different end shaped steel fiber reinforced polyester–calcite composite specimens cured at room temperature have been tested according to the four-point bending test procedure to obtain the effect of the end shapes on the mechanical properties of the composite specimens.

EXPERIMENTAL PROCEDURE

The steel wire fibers used in this study has a typical density of 7800 kg/cm^3 and an ultimate strength of 400 MPa. General purpose unsaturated polyester resin CE 92 N8 [13] is used as matrix and its specifications are listed in Table 1.

The straight-short steel fibers had a diameter of 0.5 mm and length of 20 mm for tensile testing specimens and 30 mm for four-point bending test specimens. To form the various end shaped steel wire fibers for four-point bending tests, the steel wires were cut into a length of 30 mm first, and than a pair of pliers were used to prepare them. The shapes of the fibers for four-point bending tests and their codes (hereafter simply referred to as their codes in the table) are given in Table 2.

Table 1. Liquid CE 92 N8 polyester resin properties [13].

Properties	Unit	Value of specifications
Viscosity	Cps	400 ± 60
Jell time (25°C)	min.	8 ± 2
Specific density	g/cm^3	1.2
Hardness	Barcol	Min 45
Bending strength	MPa	Min. 85
Ultimate strength	MPa	Min 45

Table 2. The codes and the types of the fibers of four-point bending composite specimens.

Fiber code	A	B	C	D	E	F
Fiber type	Matrix (no fiber)	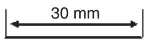	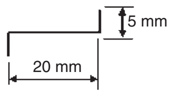	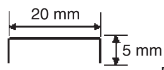		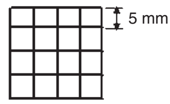

To suspend the short fibers in the uncured polyester, 14 g of calcite ($CaCO_3$) was added to 10 mL of polyester as a thickening agent before mixing with short fibers. After the calcite was added, the mixing operation continued to obtain homogeny dispersion. Cobalt Oktoat of 1% by volume was then added. The new mixture was again mixed until homogeneity was obtained. The same process was repeated after the 1% volume of methyl ethyl ketone peroxide (MERK hardener) was added. Tensile test specimens were fabricated with straight-short fibers well aligned in the longitudinal (loading) direction. For the fabrication of tensile specimens, one layer of steel wires was carefully laid into the polyester/calcite matrix, equally dividing the 5 mm thickness. On the other hand, for the fabrication of four-point bending specimens, four layers of steel wires were laid into the matrix, equally dividing the 25 mm thickness. The fiber volume fraction in all specimens was approximately 1%.

For each type of specimen, five samples were tested and their average strengths were calculated. Experimental properties measured by a Model 20000 Alsa testing machine, was revised by using a linear variable displacement transducer (LVDT) and a CODA data acquisition system. For all tests a constant cross-head displacement rate of 2 mm/min was used.

RESULTS AND DISCUSSION

Tensile Properties

The composite tensile specimens were prepared according to ASTM 638-91 standard [14], and the sketch of the tensile specimen is given in Figure 1.

In this section of the study, the unreinforced (no fiber) and straight-short fiber reinforced composite tensile specimens were manufactured at room temperature and different cure conditions of 40, 80, and 120°C for 4, 8, and 12 h. Tensile tests were performed to obtain the effect of the straight-short fibers and different curing conditions on the tensile properties of the composite specimens.

The load–displacement curves of the unreinforced and straight-short fiber reinforced composite specimens are illustrated in Figure 2. It is clearly seen that the straight-short fibers increased the load carrying capacity of the specimens. The straight-short fiber reinforced composite specimens are broken at a load of 920 N, which is greater than the unreinforced specimens by exactly 33%. In contrast to the unreinforced specimens, the load–displacement curve of the straight-short fiber reinforced specimens form a plateau after the first crack initiation. The plateau proves the effect of the straight-short fibers by means of retarding the fracture. The polyester–calcite matrix behaves as a brittle material. When the specimens are loaded step by step, the first crack is initiated through the perpendicular section of the loading direction at point I as indicated Figure 2. The crack was bridged by the fibers and a large amount of the load was transferred to the fibers between points I and II where the slope of the curve is lower. The first crack strengths of the unreinforced and the straight-short fiber reinforced composite specimen are closer to each other. It proves that the fibers do not have a salient effect on the first crack strength. Besides, the fibers prevent the catastrophic failure of the specimens. All fibers act together to carry load from point II to III because of the strong interface bonding between the matrix and the fibers. In some papers [2,4,5], it has been observed that the straight-short fiber reinforced composite specimens failed catastrophically and the stress dropped to zero after the maximum stress. In this study, some of the fibers broke at point III at a load of 920 N and then the load dropped to 540 N at point IV. From that point the fibers, except for the broken ones, continue to load bridge and pull-out gradually. Although the matrix behaves like a brittle material, the load bridging effect of the straight-short fibers is treated as a composite specimen like a ductile material.

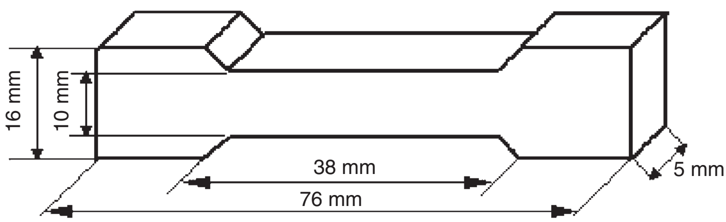

Figure 1. *The sketch of the composite tensile specimen.*

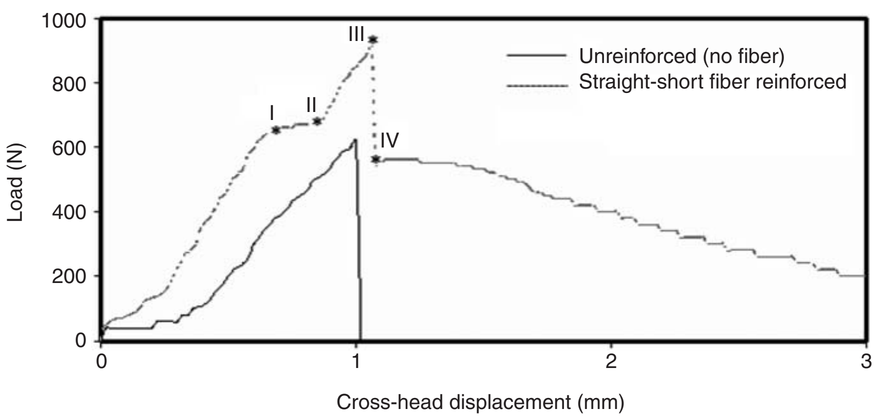

Figure 2. *Load versus cross-head displacement curves of the unreinforced (no fiber) and straight-short fiber reinforced composite specimens at room temperature.*

Figure 3 illustrates 40, 80, and 120°C cure conditions of straight-short fiber reinforced composite specimens for 4, 8, and 12 h, respectively. It can be observed from this figure that the curing temperature on the tensile properties of the composite specimens is affected. The first crack strength and the load carrying capacity of the composite specimens are increased by increasing the curing temperature for 4 h, as shown in Figure 3(a). The 120°C curing condition is more effectual on the interface bonding

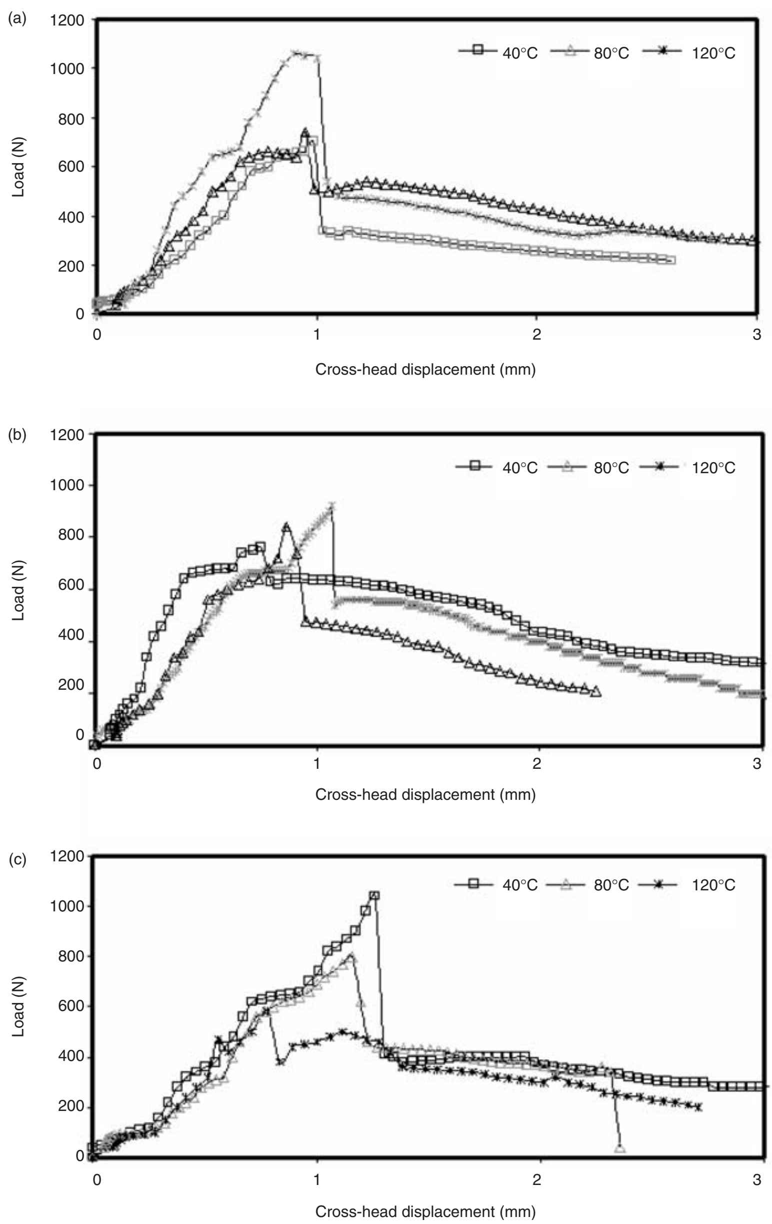

Figure 3. *Load versus cross-head displacement of composite specimens with various cure conditions: (a) 4 hour curing conditions; (b) 8 hour curing conditions; (c) 12 hour curing conditions.*

between the matrix and the fibers, because after the first crack initiation about the load of 680 N, the load carrying capacity of the 120°C cured composite specimen is increased nearly 1060 N. Additionally, all of the composite specimens similarly reach at the maximum strength at a cross-head displacement value of 0.9 mm for 4 h curing time. Comparably to Figure 3(a), the load carrying capacity of the specimens is increased by increasing the curing temperatures for 8 h as depicted in Figure 3(b). On the other hand, the first crack strength of a 40°C cured specimen is higher than the other curing conditions, and it is observed that increasing the curing temperature increased not only the maximum load carrying capacity but also increased the cross-head displacement of the composite specimens for 8 h. Contrary to Figure 3(a) and (b), first crack strength and maximum load carrying capacity of the specimens are decreased by increasing the curing temperature for 12 h as seen in Figure 3(c). The composite specimen, which is cured at 40°C, has a maximum load carrying capacity of 1030 N with maximum cross-head displacement of 1.3 mm. Like the maximum load carrying capacity, maximum cross-head displacements of the specimens are decreased gradually with increased curing temperature for 12 h.

The effect of the curing conditions on the mechanical properties of the straight-short fiber reinforced composite specimens is also realized by calculating the 'effective fiber stress analysis' using the data from Table 3. The composite specimens that were used in this study can be approximately considered as reinforced by the unidirectional fibers. Using the rule of mixture, the average fiber stress at maximum composite strength, σ_{ef}, can be described as [2,4,5]:

$$\sigma_{ef} = \frac{\left[\sigma_c - (1 - V_f)\sigma_m\right]}{V_f} \qquad (1)$$

where σ_c is the maximum composite strength (shown in Table 3), V_f the fiber volume fraction, and σ_m the maximum matrix strength. Note that the fiber volume fraction in all composite specimens is approximately 1% and the matrix strength is 12.4 MPa.

According to Table 3, the effective fiber strength of 40 and 80°C cure conditioned composite specimens are increased by increasing the curing time. In contrast to the 40 and 80°C cured specimens, the effective fiber strengths of the 120°C cure conditioned specimens are decreased with increased curing time. The effective fiber stress reaches its maximum value at 120°C for 4 h curing time. Furthermore, it is shown that the effective

Table 3. The maximum stress, (σ_c), and effective fiber stress (σ_{ef}) of straight-short fiber reinforced composites for varied curing conditions.

Curing temperature (°C)	Curing time (h)	Maximum strength, σ_c (MPa)	Effective fiber stress, σ_{ef} (MPa)
40	4	14.0	172.4
	8	16.0	372.4
	12	20.8	852.4
80	4	14.8	252.4
	8	15.2	292.4
	12	16.0	372.4
120	4	21.2	892.4
	8	16.8	452.4
	12	11.6	67.6

fiber stress of the 120°C curing condition decreases with 1.97 and 6.7 times the 8 and 12 h curing times, respectively. Additionally, it can be observed that the 12 h curing time improves the effective fiber strength 2.28 times over the 8 h curing time for 40°C curing conditions. Consequently, 12 and 4 h curing times are more effective than all other conditions for 40 and 120°C curing conditions, respectively.

Four-Point Bending Properties

The composite specimens were prepared as described above, according to ASTM 790-92 standard [15] with dimensions of $240 \times 38 \times 25\,mm^3$ for four-point bending tests. Figure 4 illustrates the test setup of four-point bending specimens.

The mechanical behavior of the A type (unreinforced) specimen resemble that of brittle materials. The maximum load of 3960 N at a displacement of 2.133 mm coincides with the first crack initiation that is propagated promptly and fails the specimen. The mechanical response of the B, C, D, E, and F type fiber reinforced composite specimens indicates some improvements on the mechanical properties over the A type specimen. An investigation on the curve of the B type fiber reinforced composite specimen just after the maximum load of 4280 N, reveals a sharp decrease of slope. This was caused by the first crack initiation and right after, the breaking of some of the fibers or pulling-out. After the first crack point, the load carrying capacity of the specimen did not continue to increase, because the matrix strength used in this study was higher than the reinforcement fibers. Due to the strong interface bonding with the matrix and the fibers, some of the fibers were broken-out with the first crack of the matrix. After the breaking of some fibers, the load continued to increase for a while owing to the other fibers that were bridging the main crack. Afterwards, the load was decreased gradually with increasing the displacement due to the fiber breakage or pull-out. A similar process was repeated again for the C, D, E, and F type fiber reinforced composite specimens. As seen from Figure 5, the load–displacement curves of composite specimens, except the A type specimens, constitute

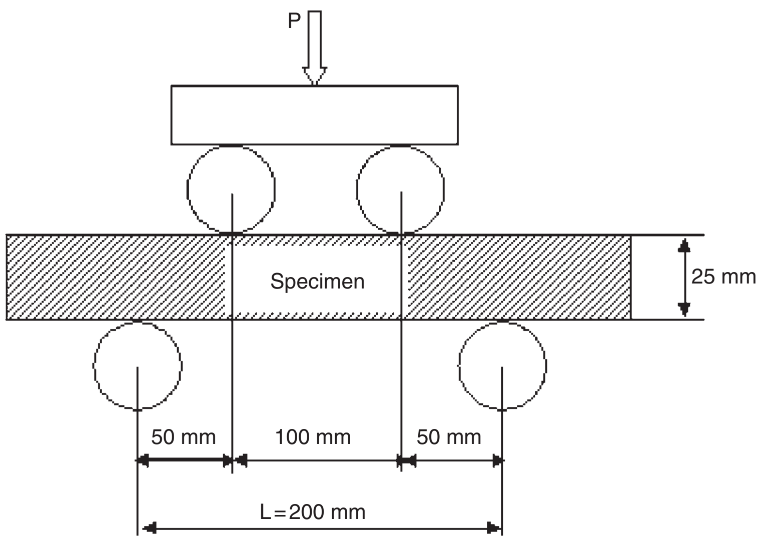

Figure 4. *Test set-up of four-point bending specimen.*

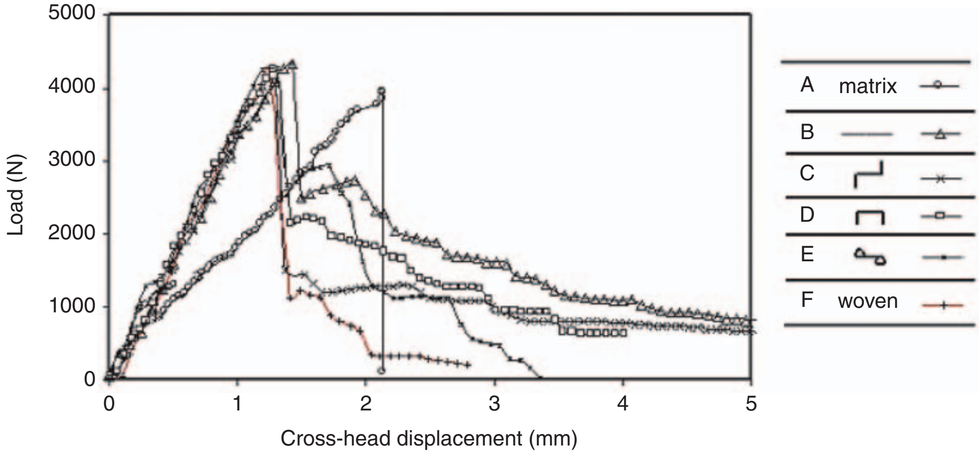

Figure 5. *Four-point bending loads versus displacement curves of the composite specimens.*

plateaus after the first crack initiation. An examination on these plateaus clearly shows that the B type fiber reinforced specimen is capable of carrying much more load compared to the other specimens. This is because the B type fibers are straight and they have more surface area embedded onto the matrix perpendicular to the cracking direction. This feature proves that B type specimens are not only better at first crack strength but also better at pulling-out properties. The worst mechanical properties is denoted by the F type fiber reinforced composite specimens. The fibers are forced to crack together by the matrix because of the woven structure. The C, D, and E type fiber reinforced specimens exhibit mechanical properties lower than the B type and higher than the F type specimens dependent on the fiber shapes.

Figure 6 compares the toughness (G) and the maximum flexural strength of the A, B, C, D, E, and F type specimens. The maximum flexural strength was calculated as [4,12];

$$S = \frac{3P_{\max}L}{4wh^2} \tag{2}$$

where $P_{\max}$ is the maximum load, L is the span length and w and h are the width and the height of the specimens, respectively. The toughness of the composite specimens was calculated from under the area of the load–displacement curves by using the MATLAB 7.0 commercial package program.

According to Figure 6, the maximum and the minimum values of toughness is calculated as 0.942 J for the B type and 0.377 J for the F type fiber reinforced specimens, respectively. Nonetheless, the toughness magnitude of the A type (unreinforced) specimen is calculated as 0.447 J, which is lower than the B, C, D, and E type composite specimens. C, D, and E type specimens have approximately the same toughness values. This is because these type of fibers have formed nearly equal lengths at the ends and they have approximately equal lengths acting on the crack bridging. Although the B type specimens have the highest maximum strength magnitude of 27.28 MPa, all other type of specimens have nearly the same maximum strength magnitudes. It is estimated that the weak mechanical properties of the reinforcement wires and the crack sensitivity of the matrix determined this result.

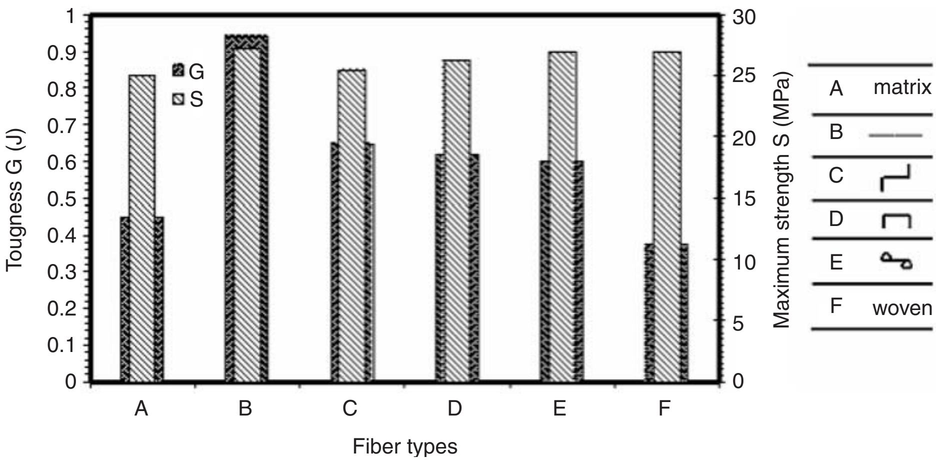

Figure 6. *Comparison of the toughness (G) and the maximum strength (S) of the composite specimens.*

CONCLUSIONS

The following remarks can summarize the tensile test results as follows:

- The straight-short fibers increase the load carrying capacity of the composite specimens exactly 33%. The load–displacement curve of the straight-short fiber reinforced specimens forming a plateau after the first crack initiation and the plateau proves the effect of the straight-short fibers by means of retarding the fracture.
- The first crack strength and the load carrying capacity of the composite specimens are increased by increasing the curing temperature for 4 and 8 h. On the contrary, first crack strength and maximum load carrying capacity of the specimens are decreased by increasing the curing temperature for 12 h.
- According to effective fiber stress calculations, 12 and 4 h curing times for 40 and 120°C curing conditions, respectively, are more effective than all other conditions.

And for four-point bending test results:

- The mechanical response of the B, C, D, E, and F type fiber reinforced composite specimens indicate improvements on the mechanical properties over the A type (unreinforced) specimen.
- Although the toughness magnitudes of B, C, D, and E type fiber reinforced composite specimens are higher than the A type (unreinforced) specimen, the toughness of the F type (woven) fiber reinforced composite specimen is lower than all other specimens.

REFERENCES

1. Liou, W. J. (1997). Stress Distributions of Short Fiber Composite Materials, *Computers and Structures*, **62**(6): 999–1012.
2. Smith, E. H. (1994). *Mechanical Engineer's Reference Book*, Oxford: Buttenworth-Heinemann.
3. Zhu, Y. T., Beyerlein, I. J., Valdez, J. A. and Lowe, T. C. (2001). Fracture Toughness of a Composite Reinforced with Bone-shaped Short Fibers, *Materials Science and Engineering*, **A317**: 93–100.
4. Zhu, Y. T., Valdez, J. A., Beyerlein, I. J., Zho, S. J., Liu, C., Stout, M. G., Butt, D. P. and Lowe, T. C. (1999). Mechanical Properties of Bone-Shaped-Short-Fiber Reinforced Composites, *Acta Mater*., **47**(6): 1767–1781.

5. Beyerleina, I. J., Zhu, Y. T. and Mahesh, S. (2001). On the Influence of Fiber Shape in Bone-shaped Short-fiber Composites, *Composites Science and Technology*, **61**: 1341–1357.
6. Zhu, Y.T. and Beyerlein, I.J. (2002). Bone-shaped Short Fiber Composites-an Overview, *Materials Science and Engineering*, **A326**: 208–227.
7. Zhu, Y. T., Valdez, J. A., Shi, N., Lovato, M. L., Stout, M. G., Zhou, S. J., Butt, D. P., Blumenthal, W. R. and Lowe, T. C. (1998). A Composite Reinforced with Bone-Shaped Short Fibers, *Scripta Materialia*, **38**(9): 1321–1325.
8. Beyerlein, J., Zhu, Y. T. and Mahesh, S. (2001). On the Influence of Fiber Shape in Bone-shaped Short-fiber Composites, *Composites Science and Technology*, **61**: 1341–1357.
9. Bagwell, R. M. and Wetherhold, R. C. (2005). End-Shaped Copper Fibers in an Epoxy Matrix—Predicted Versus Actual Fracture Toughening, *Theoretical and Applied Fracture Mechanics*, **43**: 181–188.
10. Zhou, Y., Li, C., Renaud, J. E. and Mason, J. J. (2005). Improvement of the Mechanical Properties of Bone Cement by Shape Optimization of Short Fibers, *Engineering Optimization*, **37**(2): 121–134.
11. Zhou, Y., Li, C. and Mason, J. J. (2005). Shape Optimization of Randomly Oriented Short Fibers for Bone Cement Reinforcements, *Materials Science and Engineering A*, **393**: 374–381.
12. Jiang, H., Valdez, J. A., Zhu, Y. T., Beyerlein, I. J. and Lowe, T. C. (2000). The Strength and Toughness of Cement Reinforced with Bone-shaped Steel Wires, *Composites Science and Technology*, **60**: 1753–1761.
13. Glass Fibre Co. Catalog of resine and fibre. Kocaeli, 1997.
14. Standard Test Method for Tensile Properties of Plastics, ASTM D638-91, 1991.
15. Standard Test Methods for Flexural Properties of Unreinforced and Reinforced Plastics and Electrical Insulating Materials, ASTM D790-92, 1992.